MAREK GAWOR*, JÓZEF RYSZ*

VISUALISATION OF COAL DISINTEGRATION AND INVESTIGATION OF RAPID CHANGES OF GAS PRESSURE, TEMPERATURE AND STRAIN DURING GAS-GEOMECHANICAL PHENOMENA

WIZUALIZACJA ROZPADU WĘGLA ORAZ BADANIE SZYBKICH ZMIAN CIŚNIENIA GAZU, TEMPERATURY I ODKSZTAŁCENIA PODCZAS ZJAWISK GAZOGEOMECHANICZNYCH

The paper reviews the results of experimental tests involving the disintegration of coal briquettes saturated with gas. Pressure measurements were taken on the briquette side, strain and temperature were measured inside the briquette. At the same time photos were taken of the briquette surface while it disintegrated. Application of a fast CCD camera operating in the Frame-Transfer mode allowed for recording of the emerging cracks and briquette slices and for correlating of thus obtained image with the changes of thermodynamic parameters (gas pressure, briquette deformations, temperature).

The earlier experiments revealed that the strain gauge is broken before the crack, presented in the photo, is actually formed. It can be explained by the fact that because of friction forces acting upon the side of the briquette, the disintegration process there is slower than inside the briquette. The briquette decompresses, which is registered by the strain gauges, long before it disintegrates.

At the time interval of about 2 ms all strain gauges would record the increasing deformation which indicates the briquette is decompressing before it disintegrates. At the moment of strain gauge failure, the magnitude of strain amounts to 13%. The decompression wave moves much faster than the destruction wave, reaching 80 m/s while the rate of the briquette disintegration ranges from 5 to 10 m/s. The rapid decompression wave inside the briquette facilitates gas filtration towards the free front section and "prepares" the conditions necessary for crack formation.

The motion of briquette slices formed during the destruction process is accelerated. The maximal calculated velocity of the slice motion near the briquette front is 23 m/s. Near the bottom the slices move more slowly, reaching 8 m/s. The rate of crack formation is estimated to be about 20 m/s.

The temperature changes pattern indicates that briquette cooling is an adiabatic process. At the instant the briquette breaks, the temperature changes rapidly as the result of the change of the medium in which the thermometer is placed. Most significant temperature changes occur near the briquette front where the destruction proceeds at a higher rate than near the bottom.

Key words: rock and gas outbursts, fast CCD cameras, measurement of strain and temperature in porous media

* INSTYTUT MECHANIKI GÓROTWORU, POLSKA AKADEMIA NAUK, 30-059 KRAKÓW, UL. REYMONTA 27

4

W pracy przedstawiono wyniki badań eksperymentalnych procesu rozpadu brykietu węglowego nasyconego gazem. Podczas destrukcji rejestrowano ciśnienia gazu na pobocznicy brykietu węglowego, odkształcenia i temperaturę wewnątrz brykietu, przy jednoczesnym fotografowaniu jego powierzchni. Zastosowanie szybkiej kamery CCD, pracującej w trybie Frame-Transfer, umożliwiło obserwację powstających w brykiecie szczelin i płatków oraz korelowanie zarejestrowanego obrazu ze zmianami parametrów termodynamicznych (ciśnienie gazu, odkształcenie węgla, temperatura).

W celu formowania brykietów, zamontowania przetworników pomiarowych oraz umożliwienia wykonania zdjęć zaprojektowano i wykonano rurę wyrzutową (brykieciarkę). Schemat tej rury przedstawia rysunek 2.

Do pomiaru ciśnienia gazu zastosowano piezorezystancyjne przetworniki ciśnienia firmy Lucas typ NPP-301-700A. Temperaturę mierzono za pomocą termoelementów konstantan-manganin wykonanych z drutu o grubości 0,1 mm. W celu zmniejszenia stałej czasowej termometru i zwiększenia powierzchni wymiany ciepła, rozklepano złącze czynne do grubości 10 mm. Tensometry grafitowe umieszczone wewnątrz brykietu służyły do pomiaru lokalnego odkształcenia brykietu, jak również momentu destrukcji.

Pomiar dynamicznych zjawisk zachodzących podczas wyrzutu węgla nasyconego gazem wymaga zastosowania szybkiego rejestratora sygnałów. Wykorzystano do tego celu szybki system pomiarowy oparty na dziewięciu kartach komputerowych A/C (Gawor 1999).

Wykonane eksperymenty umożliwiły: wyliczenie prędkości destrukcji brykietu (rys. 6 i 7) i prędkości ruchu płatków po oderwaniu od czoła brykietu (rys. 8 i 9), określenie grubości powstających płatków, wyznaczenie prędkości powstawania szczelin, korelację zjawisk mechanicznych — powstawanie szczelin i płatków, oraz termodynamicznych — zmiany ciśnienia gazu, odkształcenia brykietu i jego temperatury.

Na podstawie wykonanych eksperymentów stwierdzono, że rozerwanie tensometru, umieszczonego w głębi brykietu następuje wcześniej niż powstanie szczeliny widocznej na zdjęciu. Wynika to z faktu, że ze względu na siły tarcia występujące na pobocznicy brykietu proces destrukcji przebiega tutaj wolniej niż wewnątrz brykietu. Rozprężenie brykietu, rejestrowane przez tensometry, następuje dużo wcześniej niż jego destrukcja.

Wszystkie tensometry (rys. 4 i 5) rejestrują (w przedziale czasu ok. 2 ms) rosnące odkształcenie brykietu, oznaczające jego rozprężanie przed momentem destrukcji. W momencie pęknięcia odkształcenie to dochodzi do 13%. Fala rozprężenia porusza się znacznie szybciej niż fala destrukcji, jej prędkość osiąga wartość 80 m/s, a prędkość destrukcji wynosi od 5 do 10 m/s. Szybka fala rozprężenia w brykiecie ułatwia filtrację gazu w kierunku swobodnego czoła i „przygotowuje" warunki niezbędne do powstania szczeliny (Topolnicki 1999).

Tworzące się podczas destrukcji brykietu płatki poruszają się ruchem przyspieszonym (rys. 8 i 9). Maksymalna wyliczona prędkość ruchu płatków w pobliżu czoła brykietu dochodzi do 23 m/s. W pobliżu dna płatki poruszają się wolniej, maksymalna ich prędkość dochodzi do 8 m/s. Oszacowano (rys. 10), że prędkość tworzenia się szczeliny wynosi około 20 m/s.

Zmiany temperatury nie przekraczają 4 K i wskazują na adiabatyczne ochładzanie brykietu. W momencie pęknięcia brykietu następuje skokowa zmiana temperatury związana ze zmianą właściwości ośrodka, w którym znajduje się termometr. Większe zmiany temperatury następują w pobliżu czoła brykietu, gdzie proces destrukcji jest szybszy niż w pobliżu dna, gdzie jest on wolniejszy.

Zastosowanie szybkiej fotografii cyfrowej opartej na względnie taniej i równocześnie nowoczesnej kamerze CCD w istotny sposób wzbogaciło informacje na temat procesu destrukcji brykietu węglowego. Opracowano metodykę posługiwania się takimi kamerami, zarówno do badania procesów periodycznych, jak również jednokrotnych.

Słowa kluczowe: wyrzuty gazów i skał, szybka fotografia, pomiary odkształcenia i temperatury w ośrodkach porowatych

1. Introduction

Mining operations disturbing the virgin rock containing substances that undergo phase transitions may lead to rock and gas outbursts, crumps and rapid gas outflows. The monograph (Lama 1996) highlights some aspects of the problem. Rock and gas outbursts are the most complex and the most dangerous phenomena because of the effects they may produce. During such outbursts the burst — out material presents a major danger to people, machines and the excavations. At the same time huge amounts of gas are released. Rapid outflows of large quantities of gas (up to hundred thousands of cubic meters) cause the atmosphere in the mine ventilation network to become unfit for breathing. In some cases methane might be also released so there is a risk of explosion in the large areas, which endangers miners' life and renders mining operations impossible.

As in the last few years the outbursts became more frequent, more rigorous research was undertaken to explore the causes and mechanisms of outbursts. Tests are performed in laboratory conditions and *in situ*; supported by theoretical considerations (Topolnicki 1999; Gawor et al. 2000a). However, neither the basic research nor mining practice has been able to provide the objective methods of predicting the time and place of the next outbursts.

Outburst occurrences in mines negatively impact on mining activities. When a seam is classified as outburst-prone, it is necessary to measure the relevant outburst indices: intensity of desorption, coal cohesion, the amount of drillings, gas-bearing capacity of the seam and pressure. When the values of relevant indices exceed the admissible levels, certain preventive measures have to be put in place (decompressive blasting, drilling of gas outlets, watering of the seam). All these operations negatively impact on the costs of coal production. As far as Polish coal mines are concerned, gas geodynamic phenomena are most frequent in the Lower Silesia Coal Basin. The outburst hazard in the Upper Silesia Coal Basin is much lower now (Borowy et al. 1988; Kobiela et al. 1988) and it is restricted to three mines belonging to the Jastrzębska Spółka Węglowa (Coal Mining Company) S.A.: "Pniówek", "Zofiówka", "Jas-Mos". Frequent rock and gas outbursts were the reason why most collieries in the Lower Silesia Coal Basin were closed.

Because of the safety considerations, the actual investigation *in situ* of the rock and gas outbursts is impossible. That is why attempts are made to study these phenomena in laboratory conditions (mini outbursts). Most experiments are run on briquettes prepared from pressed coal powder, instead of hard coal. During the outbursts the following parameters are measured:

- pressure on the briquette side (Famin 1959; Bodziony et al. 1990; Ujihira et al. 1985; Gawor et al. 1994);
- the rate of briquette disintegration:
  - using resistors pressed into the briquette (Kravchenko 1995; Gawor, Rysz 1998),
  - using optical techniques (Gawor et al. 1994);
- briquette temperature (Gawor, Rysz 1999b);

- briquette deformation (Gawor, Rysz 1998);
- imaging of burst-out material (Bodziony et al. 1990);
- fast imaging of briquette disintegration (Ujihira et al. 1985; Gawor et al. 1994);
- outburst energy (Nelicki et al. 1994);

The investigation of the burst-out material both *in situ* and in laboratory conditions reveals that an outburst is a discrete process. The formation of the sliced structure during a rapid decompression of the porous medium is observed not only in the case of hard coal saturated with gas. Ujihira and his team investigated the outbursts in concrete where the pores were saturated with gas. Images taken during the disintegration of such material indicate that slice formation is a non-continuous process.

2. Application of CCD cameras to investigation of rapid processes

In many cases the analysis of production processes and basic research require the recording of rapid changes of process parameters. The measured physical parameters are converted into electric signals using various types of measuring sensors. The recording of electrical quantities does not involve any major difficulties since one can use fast and relatively cheap analogue to digital converters (A/D), with the sampling frequency ranging from 20 kHz to 50 MHz (Gawor 1999b).

In recent years high-speed imaging has been done with CCD cameras (Charge Coupled Device; Hiller et al. 1992a). One of the possible solution is the selection of the operating mode Frame-Transfer. The camera used for the investigation was equipped with a light-sensitive sensor TC237 made by Texas Instruments (Texas Instruments Catalogue 1996). Two surfaces of the sensor are coated with light-sensitive elements (pixels). These pixels behave similar to condensers whose charge is proportional to the intensity of incident light. The sensor matrix consists of two parts: an exposed, light-sensitive region and the covered region called the store (memory). Both matrixes have the same number of pixels: 680 along the horizontal line and 500 along the vertical line. A single pixel is a square with the side length 7.4 μm.

The Frame-Transfer mode allows for controlling the rate of image transport from one matrix to the other. Let us imagine that the image occupies only the upper section of the light-sensitive matrix while the lower part remains covered. If an object illuminated with short light pulse is captured while the sensor is exposed to light, we get the image in the 1/2 of the matrix height. Afterwards, in the precisely controlled time Δt, this image is copied line after line to the lower region of the matrix while the upper region will be blanked. Another light pulse upon the object will cause the upper section of the matrix to be lit again and this part will be again copied onto the lower section. This process can be compared to the moving film exposed to subsequent light pulses. This operating mode of the camera allows for obtaining the images picturing the four phases of the process, providing the resolution of 680 × 1000 pixels.

In the case of imaging of single or pseudo- periodical processes, the camera operations have to be synchronised with those phenomena. Thus the sensor operation is

adapted to the actual requirements so that imaging should begin at the right moment – that is exactly when the process begins (Hiller et al. 1992b). Appropriate electronic circuits controlling the camera operations were engineered by the "ARCO" company. The camera, henceforth treated as a controlled light-sensitive sensor, has the following features:

- allows for choosing the number of images in the Frame-Transfer mode: 8, 4 or 2,
- frequency of the images taken: the maximal frequency 13 330 images per second, the minimal frequency — 8 images per second,
- control of light pulse duration — from 1 µs to 65 ms,
- triggering the camera operation with external signals TTL,
- control of time delay between the external signal TTL and the first image (over the range from 0 to 16 ms, with the step 1 µs).

To implement this control system, a special program was written which has also the function providing the image display on the monitor. Furthermore, the program allows for certain image processing operations, such as fading-in, contrasting, digital filtering, gamma correlation (Russ 1992). Implementation of such features as the function correlating the intensity between selected lines or the Fourier analysis of line intensity offers new possibilities, as one can determine the slice thickness and velocity.

Let us consider now the applications of the Fourier transform to follow-up the periodic structures. In the left, lower corner in Fig. 1 a line segment comprising several slices and cracks is presented. The intensity of pixels on that segment is depicted in the upper graph. It can be seen that the intensity function reflects a certain periodic structure.
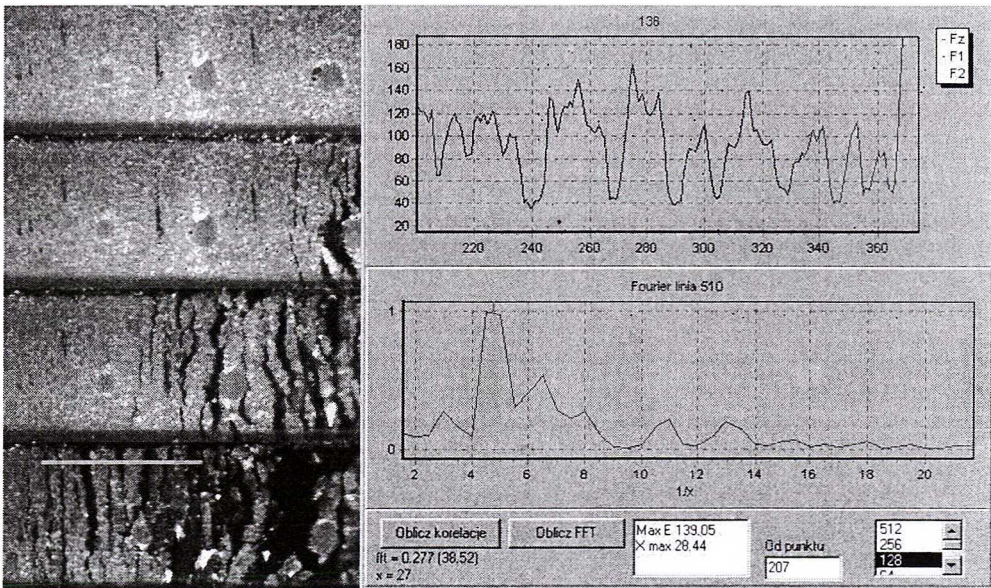

Fig. 1. Determining the slice thickness using the Fourrier transform

Rys. 1. Wyznaczanie grubości płatków za pomocą transformaty Fouriera

8

Were this function time-variant, certain characteristic frequencies could be found. The lower graph presents the Fourrier transform for the line intensity function, the maximum is found for the coordinate $x = 27$. The scale of this image is a known value, in this case one pixel corresponds to 0.042 mm, hence the slice thickness is $27 \times 0.042 = 1.1$ mm. Such analysis was applied to estimate the slice thickness at the given place.

3. The experimental set-up

A special expansion pipe was designed and made for the purpose of briquette formation and to facilitate imaging. The schematic diagram of the test pipe is presented in Fig. 2. The steel cylinder 80 mm in thickness has a smooth opening 30 mm in diameter. The pipe at one end was closed with the resistance plate (5). A hand-operated press (3) was attached at the other end. The scale (7) on the screw allowed for measurements of briquette length. The piston (2) with two O-rings on the side surface was connected to the screw by means of a ball and socket joint.

In the front section of the pipe (between the resistance plate and the briquette front) are valves (6) used to connect the vacuum pump and the gas bottle and the seat (O) of the piezoresistant transducer of free gas pressure.

On the side surface of the pipe were six seats (indicated as 0–5) for piezoresistant pressure transducers. The distance between the neighbouring seats is 24 mm, the distance between the transducers 2–4 was 12 mm. Opposite those seats are openings in which were fixed the thermocouples and graphite strain gauges.

The window (4) made from monocrystalline Al_2O_3 (corundum) of 10×30 mm size enabled observation of coal surface. The window was placed such that the axis of
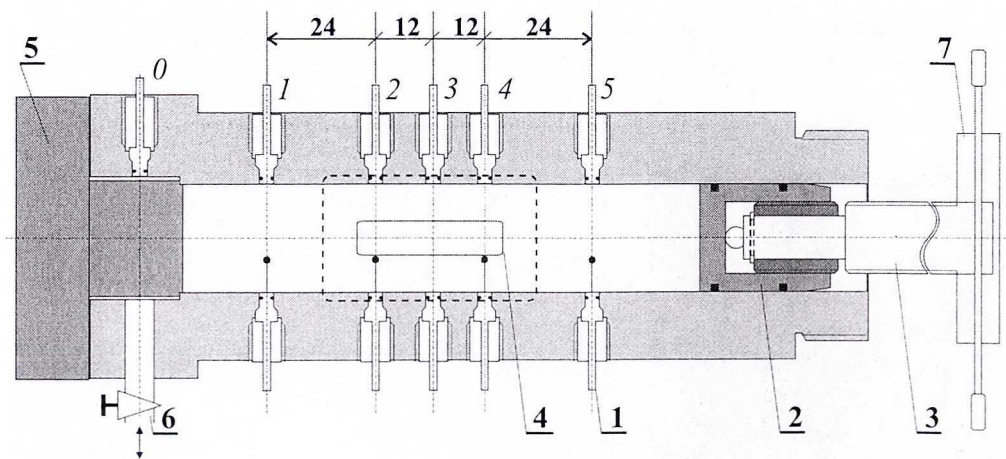

Fig. 2. Schematic diagram of the expansion pipe

Rys. 2. Schemat rury wyrzutowej

pressure transducer (3) was in the centre of visual field while the axes of transducers (2) and (4) were closely to field boundary. The are of coal surface accessible to observating was 6×28 mm. Very high strenght of corundum enabled pressing of briquette after inserting window into side surface of the pipe.

To ensure very good thermal contact between the thermocouple and the coal skeleton and to provide for homogenity in the strain gauge region, these sensors were mounted inside the expansion pipe, prior to briquette formation. After the briquette was formed, the resistance plate was removed and a copper membrane (5) was mounted (Fig. 3). The membrane was pressed to the expansion pipe via properly shaped bottom of the vacuum vessel (8). The vacuum vessel was made from the plexiglass pipe 282 mm in length and the inside diameter 195 mm. In the bottom affixed to the expansion pipe was the opening with a ring-shaped knife (6) which cut the disc 44 mm in diameter in the membrane. Cutting the membrane resulted in rapid opening of the expansion pipe. In the side surface of the vacuum vessel was the valve to provide the connection with the vacuum pump (9).
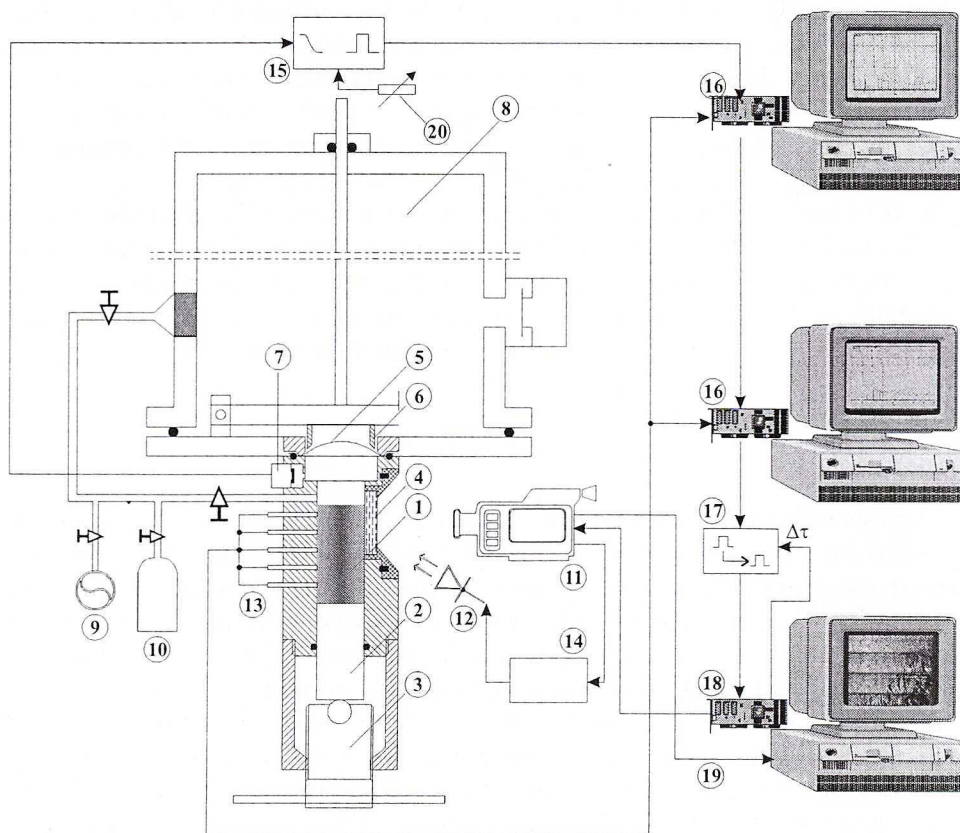
Fig. 3. The experimental set-up

Rys. 3. Schemat stanowiska pomiarowego

The only way to visualise black cracks against the black background (i.e. the briquette) was to coat the briquette surface with a light-reflecting substance. The best solution was to coat the briquette with silver lacquer having very low mechanical strength. Small droplets were deposited on the lacquered surface or scratches were made, which acted as markers identifying the position of slices.

Gas pressure was measured using the piezoresistant pressure transducers NPP-301-700A, manufactured by Lucas company. Temperature measurements were effected using thermal elements Constantan-Manganin made from wire 0.1 mm in thickness. In order to reduce the time constant of the thermometer and to increase the heat exchange area, the joint was flattened to the thickness of 10 μm. In order to measure the local briquette deformations and the moment of destruction, graphite strain gauges were placed inside the briquette (Rysz 1996). Between two metal electrodes 0.5×0.5 mm placed at the distance of 0.3 mm perpendicular to the briquette axis, some powder was put consisting of coal grains (the same coal from which the briquette was formed) with graphite segments 8 μm thick and 0.4 mm long. The whole contents were pressed during briquette formation. Coal swelling increased the distance between the electrodes, which in turn gave rise to an increase of the strain gauge resistance, while briquette breaking (a crack) stopped the electric conduction (the resistance rapidly increased to ∞).

The measurements of dynamic processes during the outbursts of coal saturated with gas require high-speed signal recorders. A high-speed measuring system using nine A/D computer cards (16) was used in this application (Gawor 1999b).

The briquette was illuminated by means of five light diodes (12). The pulse generator (14) (Stasicki et al. 1999) provided for power supply up to 5 A and the pulse time of 10 μs. Triggering the operation of the A/D card and the CCD camera from one trigger circuit allowed for synchronisation of voltage measurements and the instant of image taking. In some experiments the delaying circuit had to be used (17).

4. Results

As it was mentioned in the previous sections, the main objective of the research was to prepare the measuring stand allowing for simultaneous imaging and recording of thermodynamic parameters when the briquette disintegrated. Experiments were run at the saturation pressure about 0.70 MPa. Decompressing gas expanded to the tank (the vacuum vessel (8) — Fig. 3) whence it was pumped out to bring the pressure down to the order of several Pa. Briquettes were saturated with helium or carbon dioxide and pressed till the geometric porosity would be 20 or 24%. Porosity was obtained from the geometric dimensions of the briquette and the real density of coal (1.61 g/cm^3).

The imaging frequency ranged from 1900 to 13 000 images per second. The time delay between the triggering signal and actual imaging was also varied (from 0 to 2.2 ms). Placing the briquette bottom or the front part within the display window allows for recording of subsequent phases of briquette disintegration. In the experiments in which the briquette front could be seen in the window, the signal triggering the card and

the camera came from the pressure transducer measuring the free gas pressure ahead of the briquette front. In the experiments in which the briquette bottom could be observed in the window, the triggering signal would come from the pressure transducer lying on the plane 2, that is near the edge of the window.

, To facilitate image examination, the following information is provided: on the left — the time axis (time measured from the instant the triggering signal arrives); on the right — image number (the image indicated with 0 was taken before the experiment); at the bottom: briquette position with respect to the window and the arrangement of measuring sensors; at the top: the arrows bearing the numbers 2, 3, 4 indicating the position of sensors. The time step between the subsequent images are also provided.

4.1. Correlation of place and time of briquette disintegration on the basis of images and strain gauge failure

An experiment was run on coal with the porosity was 20%. Images were taken at the rate of 3080 images per second (0.33 ms). The briquette was saturated with helium at the pressure 0.75 MPa, it was then decompressed to reach the vacuum. The briquette front was in the window, 0.5 mm from its right edge and 0.9 mm to the right of the measuring plane 2.

The strain gauge failure (Fig. 4) in the plane (2) occurs at the moment the triggering signal arrives, actually it is exactly 0.04 ms before that signal. In the first image taken in the 10th ms the briquette seen against this plane is cracked and the crushing surface extends to the spot distant by 2.0 mm from the briquette front. In the measuring plane 3, that is in the briquette middle section, there was no strain gauge. That is not an intended result, however. The strain gauge placed in that position broke during the pressing of subsequent briquette sections because of coal displacement. Let us consider the behaviour of the strain gauge 4 in the measuring plane in the left side of the window (at the distance of 24 mm from the plane 2). Briquette decompression begins much earlier than briquette disintegration. The strain gauge registers the briquette disintegration at the instant $t = 1.85$ ms, that is between the sixth and seventh image. In the sixth image the crushing wave is 9.5 mm ahead of the strain gauge in the position 4, at that time the strain gauge registers the deformations amounting to 7.5%. In the seventh image we can see cracks confirming briquette disintegration.

As it was mentioned earlier, in other experiments the briquette front was 48 mm from the window while the briquette end section was within the field of camera vision. The main objective of these experiments was to examine the final stages of briquette disintegration, that is when the process is slowed down. Fig. 5 depicts the disintegration of the briquette with the porosity 20% saturated with carbon dioxide at the pressure 0.71 MPa. The imaging frequency was 0.525 ms, at the rate of 1900 images per second. The triggering signal came from the pressure transducer fitted in the measuring plane 2. The first image was taken at the instant when the pressure on the side surface of the briquette, in the measuring plane in the near the window edge, was 0.65 MPa.
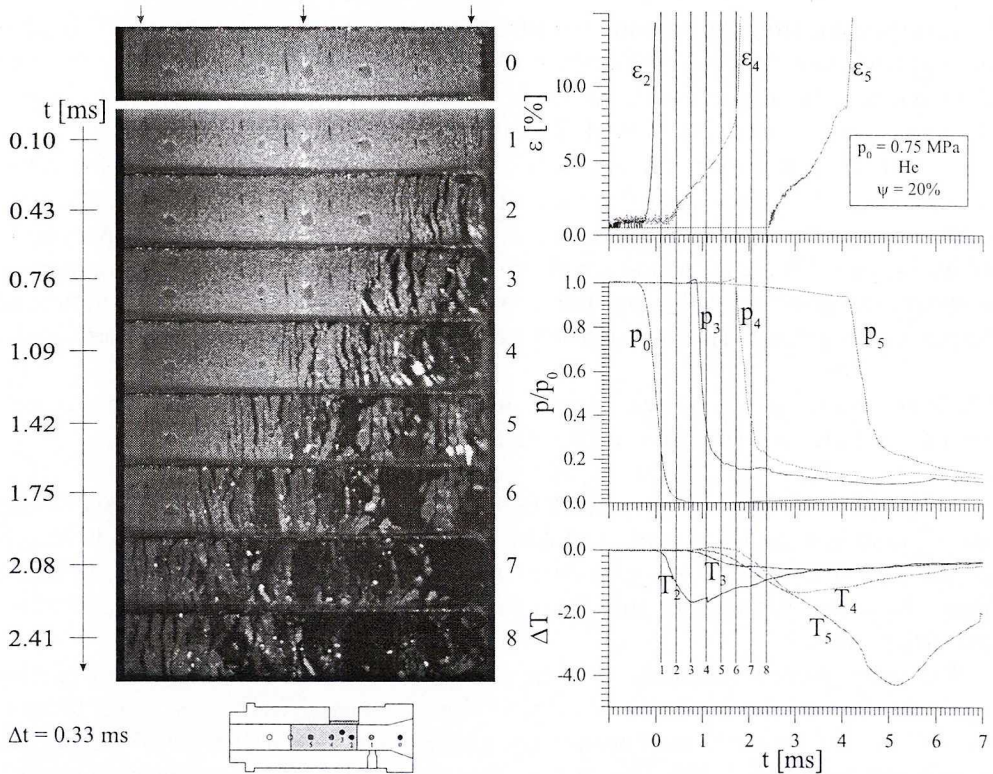
12

Fig. 4. Briquette disintegration (near the front section) and variations of strain, pressure and temperature in the experiment with a briquette having the porosity 20%, saturated with helium

Rys. 4. Zdjęcie rozpadu brykietu (w pobliżu czoła) i zmiany odkształceń, ciśnień i temperatur w eksperymencie, w którym brykiet o porowatość 20% nasycono helem

The strain gauge in the measuring plane 2 broke at the instant the first image was taken, then the gas pressure decreased rapidly. In this image we can see the crack 5.1 mm from the right edge of the window. The strain gauge in the middle part of the window (plane 3) breaks right before the fourth image is taken and the rapid pressure drop occurs a fraction of a millisecond later. In the fourth image the crushing wave reaches that plane — we can easily see a crack in this plane.

The strain gauge in the measuring plane 4 (4 mm from the briquette bottom, along its axis) breaks before the sixth photo is taken, when the crushing wave (near the window surface) reaches the spot 13 mm from the strain gauge. In the image 7 we sees distinct cracks that propagates to the plane 4 — after that the gas pressure falls rapidly. Considerable delay in the strain gauge (4) failure time and the pressure drop lead us to suppose that the surface of the crushing wave in the final briquette section is cone-shaped. That is borne out by numerous experiments where after an outburst we find a ring-shaped layer of coal adhering to the side surfaces.
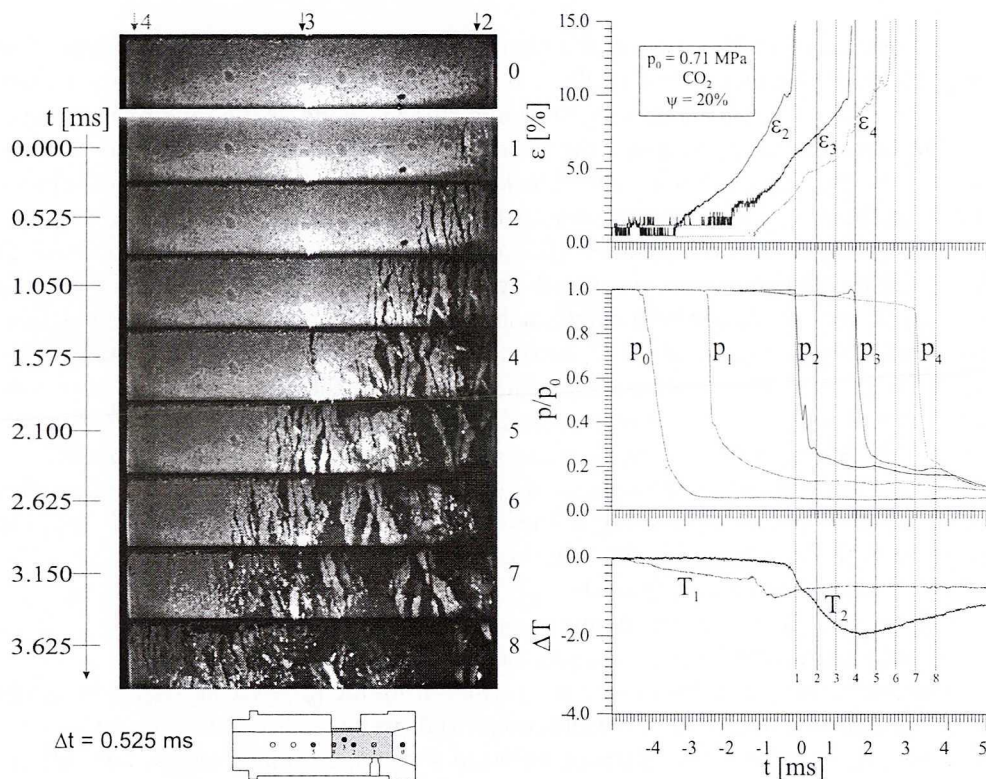
Fig. 5. Briquette disintegration (near the bottom) and the changes of strain, pressure and temperature
in the experiments with the briquette having the porosity 20% saturated with carbon dioxide

Rys. 5. Zdjęcie rozpadu brykietu (w pobliżu dna) i zmiany odkształceń, ciśnień i temperatur
w eksperymencie, w którym brykiet o porowatość 20% nasycono dwutlenkiem węgla

The velocity of the crushing wave between the third and fourth image is increasing. This is due to briquette heterogeneity in the spot the strain gauge was pressed- in. That is the spot where two parts of the briquette are "glued" together, as it is necessary to place there a strain gauge and a thermometer. The eighth image, on the left side of the window depicts the briquette bottom and the phase of disintegration right before reaching the bottom. At that moment the process of disintegration is slowed down and thus formed slices are getting thinner.

4.2. Determining the rate of briquette disintegration

It is relatively easy to determine the rate of briquette disintegration using the imaging techniques. It is sufficient to find the last formed crack in the subsequent images. In order to do that, we move the mouse cursor to the crack and read out its position. When we input the image scale to the program (pixels recalculated into millimetres), we get

crack position in millimetres. In the same manner we determine the position of the briquette front. Knowing the time delay between the images, we can plot the diagrams $x - t$ (position of the disintegrating portion of the briquette vs the time of imaging).

The moments of strain gauge failure may be superimposed on thus prepared diagrams. The moment the strain gauge breaks can be read out through moving the mouse cursor in the program for control and analysis of A/D cards.

Basing on the research program (Gawor et al. 1999a) covering the impacts of the dead volume of the pressure sensor on the waveform of the signal generated by the rapid pressure change in the porous medium, it is assumed that the breaking of coal will result in a rapid drop of gas pressure. At the time when the given function changes its value very rapidly, its time derivative assumes its extremum value. The derivative of pressure with respect to time was determined and the function minimum was sought (Litwiniszyn 1997). Fig. 6 depicts the diagrams $x - t$ obtained in the experiment presented in Fig. 4. Points representing the instants of crack formation, rapid pressure falls and strain gauge failures lie along the straight lines. The inclination of those straight line is the measure of the disintegration rate. Thus obtained rates are as follows:

- obtained from image analysis: $v_z = 12.1$ m/s,
- obtained from briquette deformations: $v_o = 11.2$ m/s,
- obtained on the basis of pressure drops $v_p = 10.4$ m/s.

The rate of briquette disintegration obtained from the image analysis is higher than that calculated on the basis of deformations and pressure. We have to bear in mind, however, that the base (the distance between sensors) in image analysis is different than in pressure and strain measurements. In the case of images, the average rate of disintegration is obtained for the whole path of 26 mm, starting from the briquette front. In the case of pressure and strain measurements the average rate is calculated for the
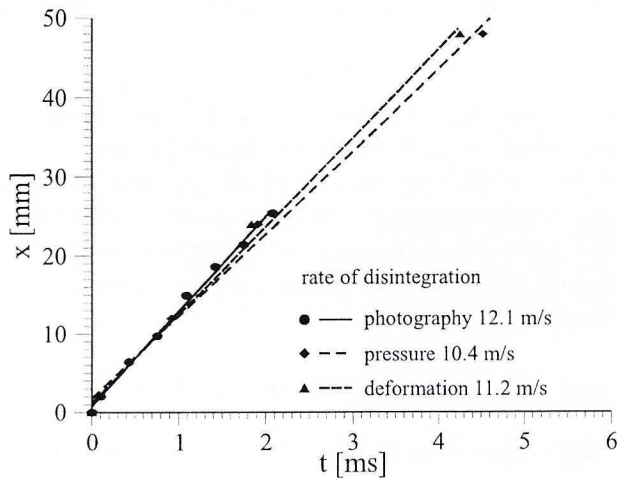

Fig. 6. The rate of briquette disintegration in the early stage of the process

Rys. 6. Prędkość destrukcji brykietu w początkowej fazie procesu

whole briquette length (48 mm). The fact that the disintegration rate v_z is greater than v_o indicates that in the initial section of the briquette the disintegration process is faster. The difference between the velocity v_o and v_p bears out the notion that the disintegration process is slowed down on the briquette side surface because of the friction forces between the briquette and the walls of the expansion pipe.

The next diagram $x - t$ (Fig. 7) depicts the phase of briquette crushing during the experiment where the briquette bottom could be observed through the window (Fig. 5). The measurement points do not form straight lines as exactly as in Fig. 6. They follow a curve pattern, the curve inclination gradually decreasing. The rates of disintegration obtained from this diagram are as follows:

- obtained from image analysis: $v_z = 5.4$ m/s,
- obtained on the basis of pressure drops — over the whole briquette $v_p = 8.5$ m/s,
- obtained on the basis of pressure drops (in the window region) $v_{po} = 5.9$ m/s.
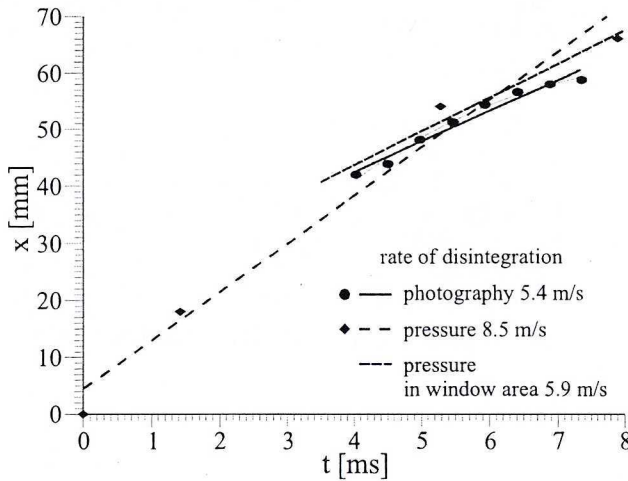

Fig. 7. The rate of briquette destruction in the final stage of the process

Rys. 7. Prędkość destrukcji brykietu w końcowej fazie procesu

In the end section of the briquette the disintegration process is slower. The delay obtained on the basis of the parabola arc fit to the measurement points (image analysis) is -0.9 m/s^2. The disintegration process is slowed down right before the bottom section is reached, as it can be seen in Fig. 5. Thus formed slices are thinner and move more slowly.

4.3. Determining the velocity of slices

As it can be seen in Figs. 4 and 5, there are brighter patches on the briquette surface that allow for observation of slice movements (they act as markers). The $x - t$ diagrams can be plotted for the markers too, as it was done to analyse the crushing wave. Two

16

examples will be provided to present the case when the briquette front is observed (Fig. 8 on the basis of Fig. 4) and when the bottom is under scrutiny (Fig. 9 on the basis of Fig. 5). Velocities of slice motion provided in these diagrams were calculated from the displacement between their positions on two subsequent images. On the left side are the initial positions of analysed markers provided on the briquette surface.
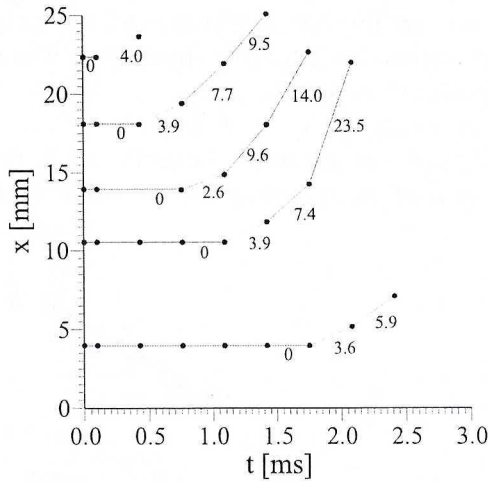

Fig. 8. Slice motion near the briquette front (the numbers indicate the local velocity of slices in m/s)

Rys. 8. Ruch płatków w pobliżu czoła brykietu (liczby oznaczają lokalną prędkość płatków w m/s)
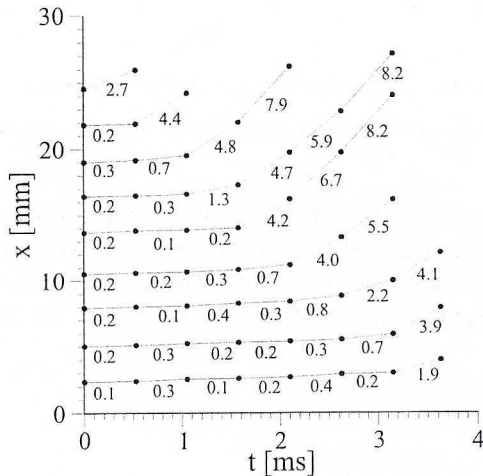

Fig. 9. Slice motion near the briquette bottom (the numbers indicate the local velocity of slices in m/s)

Rys. 9. Ruch płatków w pobliżu dna brykietu brykietu (liczby oznaczają lokalną prędkość płatków w m/s)

It can be seen that the slice motion is accelerated. Soon after their separation from the briquette, the slices move at about 4 m/s no matter whether we observe the slices near the briquette front or bottom. In the initial phase of the disintegration process (the briquette front) the slices accelerate more considerably than during the final stage (near the bottom). The maximal velocity of the slice motion reaches 23 m/s. In the final stage, when the disintegration process is slowed down, the maximal velocity of the slice motion is only 8 m/s. That confirms the notion (also verified by image analysis) that in the final stage of disintegration the forming slices are "removed" more slowly so they do not move so fast.

There is a major difference between the two diagrams. When we observe the briquette front we do not encounter the previous displacements of markers. Markers will change their position at the instant of briquette disintegration. The situation is quite different when we consider the disintegration of the briquette bottom. All the markers get shifted before the crushing wave ever reaches them. The velocity of their motion is about 0.2 m/s. Let us see now how the strain gauge near the briquette bottom (2.5 mm from the bottom), in the measuring plane 4, should behave (Fig. 4). This strain gauge begins to deform 1 millisecond before the first image. Right before the moment of disintegration, the strain gauge deformation would reach 13%. That suggests that the velocity of the decompression wave in the coal skeleton is much greater that of the destruction wave.

4.4. Formation of cracks and the sliced structure

Experiments were run to check whether images taken at the maximum speed of camera operation would allow for determining the rate of crack formation. Tests were run on a briquette having the porosity 20%, saturated with carbon dioxide at the pressure 0.73 MPa. The imaging frequency was 13 330 images per second, that is every 0.075 ms. The camera and signal recording system were triggered by the pressure drop on the pressure gauge in the middle section of the window (the measuring plane 3).

The images obtained in this experiment are shown in Fig. 10. The local velocity of the crushing wave measured over the distance of 4.3 mm in the middle section of the window obtained on the basis of images was $v_z = 8.7$ m/s. The velocity of slice motion after their separation from the briquette body was 6.6 m/s. This velocity was obtained from the position of the fifth marker patch (counting from the left). In the later phase the sixth patch distant from the undisturbed briquette section by about 20 mm (in the photo) moves with much higher velocity: 11.8 m/s.

The process of crack formation is rather complex. The analysis of crack formation is rendered still more difficult by the changes of light reflected from the surface of the crushed briquette and by the narrow field of vision. The change of light reflexes occurs as the slices move away from the window surface and rotate round the briquette axis. The cracks do not form planes exactly perpendicular to the briquette axis. During the initial phase the cracks are widened, sometimes they are patched up by newly formed slices. It can be well seen in enlarged fragments of the photos 6, 7, 8 (Fig. 10). In the sixth
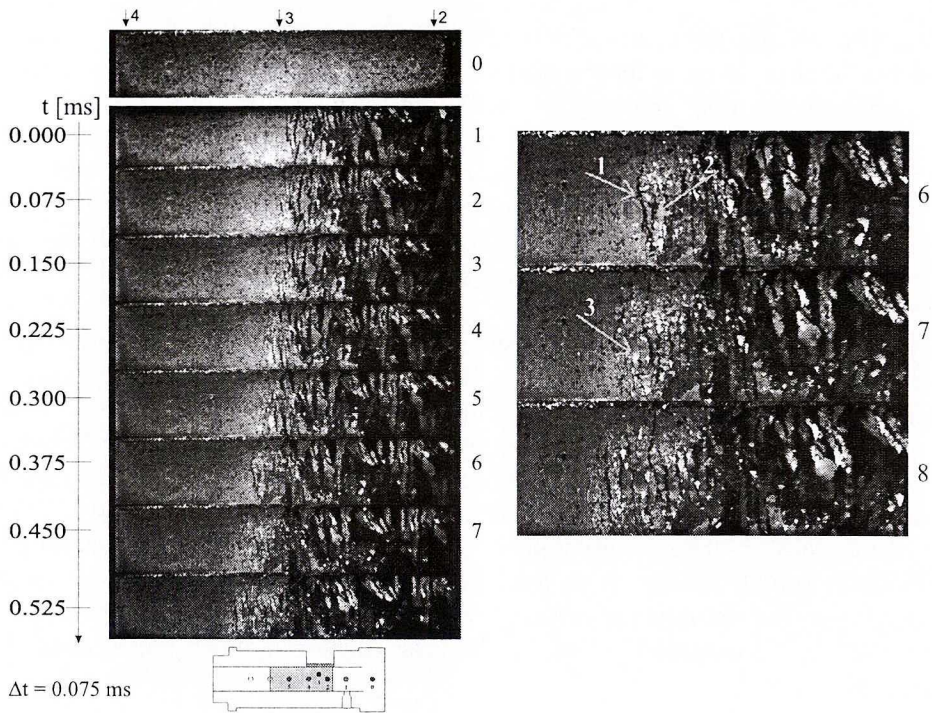
18

Fig. 10. Process of grows of cracks

Rys. 10. Zdjęcia rozpadu brykietu obrazujące proces tworzenia szczelin (z prawej strony powiększenie)

photo the last crack separating the disintegration front (indicated with an arrow 1) is thicker than in the seventh photo. That suggests the slice motion is not uniform, some of them may move faster than others.

This imaging frequency makes it impossible to answer the question how the cracks are formed. We can easily see that some cracks are elongated. In the sixth photo a small crack, in the middle section, is indicated with the arrow 2. The initial length of this crack was 1.3 mm. In the seventh photo the crack has about 2.8 mm in length. We can thus estimate the rate of this crack elongation $v_{sz} = (2.8 - 1.3)/0.075 = 20.0$ m/s.

The formation of a crack passing through the marker centre indicated with an arrow (3) in the seventh photo is an extremely interesting process. In the sixth photo there is no crack on the marker, though a brighter line in its middle section can be observed. This line changes into a crack in the seventh photo while in the eighth one the crack expands.

The rate of crack shift is approximately equal to the slice velocity. The newly — formed slices have an irregular shape and during their movement they further disintegrate. It is extremely difficult to determine their thickness. We can only say that immediately after they separate from the briquette, their thickness may vary from 0.3 to 1.0 mm.

We notice as well that slice movements are faster in the middle sections of each photo. That is because the friction force between the corundum window and the steel briquette pipe may vary in magnitude (the upper edge of each photo is the boundary line between corundum and steel).

4.5. Temperature changes

The patterns of temperature decrease observed in the experiments (Figs. 4 and 5) indicate that the briquette cooling is an adiabatic process. The early phase of the temperature drop is fairly well correlated with the beginnings of briquette deformations. Temperature increases after the briquette disintegrates because some heat is imparted by the surroundings.

A detailed analysis of the temperature signal (curve T_5, see Fig. 4) reveals that at the instant the strain gauge breaks (i.e. at the moment of briquette disintegration), the temperature decrease is slowed down. That is the instant when the properties of the medium undergo a rapid change. At the beginning the thermocouple measures the temperature of coal when the briquette is decompressed. Then the temperature decrease is slowed down for a very short time (about 0.3 ms) because the temperature is now measured in a slice separated from the decompressed briquette. Another rapid temperature decrease is caused by the fact that the thermal element measures the temperature of expanding mixture of gas and tiny coal fragments.

As the temperature changes are caused by adiabatic decompression of the briquette saturated with gas, the maximal drop of temperature depends on the rate of this process. In the experiments where the initial stages of briquette decompression were observed the rate of strain gauge deformation was about 5%/ms. The rate of disintegration wave in those experiments was about 10 m/s. The maximal temperature decrease was — 4 K. In case when the process of briquette disintegration near the bottom was observed, the rate of strain gauge deformation would be smaller, nearing 3.5%/ms. The maximal deformation was 13% over the period of 3.5 ms. The rate of disintegration was about 6 m/s. The maximal temperature decrease registered in this case was about — 2 K.

5. Conclusions

Application of high-speed digital imaging using relatively cheap yet modern CCD cameras is a simple way to improve our understanding of the process of coal briquette disintegration. The methodology of using those cameras was developed so that they can be used in investigation of both periodic and single processes.

These cameras can be also used for flow visualisation in liquids. Special tracing techniques can be applied whereby one image is taken at the precisely determined, long flash time and we get the traces of segments of trajectories of particles suspended in liquids. The cameras may be also applied to the PIV method (Particle Image Velocimetry), which consists in taking two images, with a specified time interval. Then

the same fragments are compared to determine the velocity field. The methods can be also applied to determine most complex velocity fields, such as vortices or flows at the changing profiles.

The application of digital techniques of image analysis, such as Fourrier analysis or the correlating function offer new interpretations of experimental results.

The most frequently applied methods of measuring the rate of briquette disintegration involves measuring the pressure drops on the side surface of the briquette (Gawor et al. 1996). An assumption is made that the pressure falls at the moment when the briquette is broken and a slice is formed. However, some experiments reveal that it is extremely difficult to precisely determine the instant of pressure decrease. That is why other methods are used to determine that moment, including the calculation of the time derivative and assuming its minimal value is reached at the moment of passing of the front of the destruction wave.

The measurements of the disintegration rate may be inaccurate for other reasons as well: because of the friction forces the briquette properties on the side surface may differ from those along its axis. The observations of the outbursts cavern seem to bear out the notion that whenever the briquette was not entirely destroyed the cavern would be conical in shape as along the briquette axis the amount of the burst-out material is greater than on the side surface.

This observation is confirmed by measurements taken with strain gauges pressed in the coal powder before the briquette is formed and placed along the briquette axis. The strain gauge failure and hence the briquette destruction comes first along the axis, earlier than on the side surface (Rysz 1997).

The experiments lead us to suppose that the strain gauge failure occurs before a crack seen in the photo is formed, as because of the friction forces acting upon the side surface of the briquette the disintegration is slightly delayed with respect to the briquette interior. Briquette decompression, registered by the strain gauges, takes place much earlier that its disintegration.

Because of briquette heterogeneity being the consequence of the formation process (strain gauges and thermometers have to be placed in the middle section of the briquette), the local variations of the disintegration rate may occur. This change of the briquette disintegration rate is seen both in the images and can be inferred from the deformation patterns.

During the initial phase of briquette disintegration (near the front), the rate of the process is much higher than near the bottom.

Slices formed during the briquette disintegration move with the accelerated motion. The maximal velocity of briquette slices, near the front part, can be as high as 23 m/s. Near the bottom the slices move more slowly, their maximal velocity reaches 8 m/s.

In case when the briquette front is under observation, the markers do not shift their position before the disintegration process begins. When we investigate the behaviour of the bottom part of the briquette the situation is quite different. All markers are shifted before the crushing wave reaches them. The rate of their motion is about 0.2 m/s.

The behaviour of the strain gauge near the briquette bottom is an interesting point, too. The strain gauge begins to deform 1 millisecond before the first image. Right before the moment of disintegration the magnitude of deformation rate is as high as 13%.

During the initial phase of their motion, the slices move in a haphazard manner, either widening or filling-in the cracks.

The rate of crack formation was estimated to be about 20 m/s.

The pattern of temperature changes suggests that briquette cooling is an adiabatic process. At the instant the briquette breaks, the temperature changes rapidly as the result of the change of the medium in which the thermometer is placed. Most significant temperature changes occur near the briquette front where the destruction proceeds at a higher rate than near the bottom.

REFERENCES

Bodziony J., Nelicki A., Topolnicki J., 1990: Investigations of experimental generation of gas and coal outburst. In Strata as Multiphase Medium. Rock and Gas Outburst. Ed. J. Litwiniszyn, Kraków, vol. II, 489–509.

Borowy B., Michalik H., Nawrat S., Stobiński J., 1988: Kształtowanie się zagrożenia wyrzutami metanu i skał w kopalniach Rybnicko-Jastrzębskiego Gwarectwa Węglowego oraz niektóre metody jego zwalczania. Referat na XII Międzynarodowym Kolokwium „Kierunki Zwalczania Zagrożenia Wyrzutami Gazów i Skał w Górnictwie Podziemnym". Nowa Ruda–Radków, vol. I, 321–343.

Famin L.B., 1959: Instantaneous outburst of coal and gas in laboratory experiment. [In:] Problemy rudnichnoi aerologii, Gosgortekhizdat, Moscow.

Gawor M., Kowalewski T., Rysz J., Smolarski A., 1994: Experimental research on briquette destruction caused by rarefaction waves. Archives of Mining Sciences 39 (3), 313–330.

Gawor M., Rysz J., Rachalski A., 1996: Lokalny pomiar ciśnienia gazu w porach oraz temperatury i odkształcenia brykietu węglowego podczas wyrzutu. [W:] XXVIII Międzyuczelniana Konferencja Metrologów. Częstochowa, 23–25 wrzesień. Materiały konferencyjne t. 1, s. 150–155.

Gawor M., Rysz J., 1998: Badanie mechanizmu rozpadu brykietu węglowego. Materiały Konferencji Naukowej „Zjawiska fizyczne w wielofazowym ośrodku skalnym", IMG PAN, 97–114.

Gawor M., Rysz J., Palacz J., 1999a: Badanie właściwości metrologicznych miniaturowych przetworników ciśnienia. Prace IMG PAN, Kraków, 11–22.

Gawor M., Rysz J., 1999b: Dynamic phenomena accompanying sudden outburst in coal briquette. Proc. 8st Int. Symp. on Mine Plan., Dniepropetrovsk, 231–238.

Gawor M., 1999: Karta szybkiego przetwornika analogowo cyfrowego z oprogramowaniem. Metrologia i Systemy Pomiarowe VI (4) 249–255.

Gawor M,. Litwiniszyn J., Rysz J., Smolarski A.Z., 2000a: Rock and Gas Outbursts. Archives of Mining Sciences 45 (3), 347–361.

Gawor M., Rysz J., 2000b:. Zastosowanie kamery CCD do badania szybkich procesów pojedynczych i periodycznych. Prace Instytutu Mechaniki Górotworu, PAN, Kraków.

Hiller W.J., Kowalewski T.A., Tatarczyk Th., 1992a: High speed imaging with a frame-transfer CCD. Int. Cong. High-Speed-Photogrphy Victoria, Canada, 21–25 Sept.

Hiller W.J., Kowalewski T.A, Llorachforner V., Steuckrad B., Behnia M., 1992b: Charge-coupled devices in flow Visualization. 6th Int. Flow Visualization Symp. Yokohama, 5–9 Oct.

Katalog Texas Instruments, 1996.

22

K o b i e l a Z., K r z y s z t o l i k P., Z a w i e r u c h a M., 1988: Strefy wysokiej metanonośności a zagrożenie wyrzutami metanu i skał w pokładach węgla Górnośląskiego Okręgu Przemysłowego. Referat na XII Międzynarodowym Kolokwium „Kierunki Zwalczania Zagrożenia Wyrzutami Gazów i Skał w Górnictwie Podziemnym". Nowa Ruda–Radków, vol. I, 239–257.

K r a v c h e n k o V.S., 1955: On the nature and mechanism of sudden outburst of gas and coal. Iz. AN SSSR, Otd. Tekhn. Nauk. No 6, 101–108.

L a m a R.D., B o d z i o n y J., 1996: Outburst of gas, coal and rock in undeground coal mines. R. D. Lama & Associates, Wollongong, NSW, Australia.

L i t w i n i s z y n J., 1997: Model inicjacji wyrzutu mas skalno-gazowych. Sprawozdanie z projektu badawczego, Nr ST 12A02908, IMG PAN.

N e l i c k i A., T o p o l n i c k i J., 1994: Experimental stand for the investigations of outbursts of porous materials saturated with gas. Archives of Mining Sciences, vol. 39, (3), 301–311.

R u s s J.C., 1992: The Image Processing Handbook. CRC Press. Inc. Boca Raton, Florida.

R y s z J., 1996: Strain gauges for rock outburst studies. MST News Polad. 4.

R y s z J., 1997: Measurement of local values of strains of the briquette by means of special resistance strain gauges. [In:] Proc. SPIE — The International Society for Optical Engineering. Optoelectronic and Electronic Sensors II. Szczyrk, 13–16 May 1996, vol. 3054, s. 118–121.

S t a s i c k i B., H i l l e r W.J., M e i e r G.E.A., 1990: Light pulse generator for high speed photography using semiconductor devices as a light source. Optical Engineering 27 (7), 821–827.

T o p o l n i c k i J., 1999: Wyrzuty skalno-gazowe w świetle badań laboratoryjnych i modelowych. IGSMiE PAN, Kraków.

U j i h i r a M., H i g u c h i K., N a b e y a H., 1985: Scale model studies and theoretical considerations on the mechanism of coal and gas outburst, Proc. 21st Int. Conf. Of Safety in Mines Res. Inst., Sydney, NSW, 121–127.